greater for Os than for Ru ($5d_{Os}$ vs. $4d_{Ru}$), indicates that the coupling between sites is dominated by Ru^{II}–bridging-ligand mixing, as assumed in the treatment of Richardson and Taube.[26] Therefore, the effects of delocalization for the structurally analogous Ru^{II}–Ru^{III} and Ru^{II}–Os^{III} dimers should be roughly the same. A last point is that α^2 is small, supporting the assumption that electrostatics and solvation energies provide the dominant factors in determining the magnitude of $\Delta(\Delta E_{1/2})$.

Acknowledgment is made to the Army Research Office—Durham, under Grant No. DAAG29-82-K-0111, for support of this research.

(26) Richardson, D. E.; Taube, H. *J. Am. Chem. Soc.* **1983**, *105*, 40.

Registry No. $[(bpy)_2ClRu(4,4'\text{-bpy})OsCl(bpy)_2](PF_6)_2$, 91128-12-0; $[(bpy)_2ClOs(4,4'\text{-bpy})]PF_6$, 91190-06-6; *cis*-$(bpy)_2RuCl_2$, 19542-80-4; $[(bpy)_2Ru(bpm)](PF_6)_2$, 65013-23-2; $[(bpy)_2Ru(bpm)Ru(bpy)_2](PF_6)_4$, 65013-25-4; $[(bpy)_2Os(bpm)](PF_6)_2$, 91157-03-8; *cis*-$(bpy)_2OsCl_2$, 79982-56-2; $[(bpy)_2Ru(bpm)Os(bpy)_2](PF_6)_4$, 91128-14-2; $[(bpy)_2Ru(pyzc)]PF_6$, 91128-16-4; $[(bpy)_2ClRu(pyzc)Ru(bpy)_2](PF_6)_2$, 91128-18-6; $[(bpy)_2Os(pyzc)]PF_6$, 91128-20-0; $[(bpy)_2ClRu(pyzc)Os(bpy)_2](PF_6)_2$, 91128-22-2; $[(bpy)_2ClRu(pyz)RuCl(bpy)_2](PF_6)_2$, 91128-23-3; $[(bpy)_2ClRu(pyz)OsCl(bpy)_2](PF_6)_2$, 91128-25-5; $[(bpy)_2ClRu(4,4'\text{-bpy})RuCl(bpy)_2](PF_6)_2$, 49734-40-9; $[(bpy)_2ClRu(pyz)RuCl(bpy)_2](PF_6)_3$, 91128-27-7; $[(bpy)_2ClRu(pyz)OsCl(bpy)_2](PF_6)_3$, 91128-35-7; $[(bpy)_2ClRu(4,4'\text{-bpy})RuCl(bpy)_2](PF_6)_3$, 91128-29-9; $[(bpy)_2ClRu(4,4'\text{-bpy})OsCl(bpy)_2](PF_6)_3$, 91157-05-0; $[(bpy)_2Ru(bpm)Ru(bpy)_2](PF_6)_5$, 91128-31-3; $[(bpy)_2Ru(bpm)Os(bpy)_2](PF_6)_5$, 91128-37-9; $[(bpy)_2ClRu(pyzc)Ru(bpy)_2](PF_6)_3$, 91128-33-5; $[(bpy)_2ClRu(pyzc)Os(bpy)_2](PF_6)_3$, 91128-39-1.

Contribution from the Department of Chemistry, North Carolina State University, Raleigh, North Carolina 27650

Unique Redox and Spectroscopic Properties of Dipyridylamine Complexes of d^6 Transition Metals: Electrochemical Behavior

DAVID E. MORRIS, YASUHIKO OHSAWA, DONALD P. SEGERS, M. KEITH DeARMOND,* and KENNETH W. HANCK*

Received November 2, 1983

Room- and low-temperature cyclic voltammetric and spectroscopic results in CH_3CN are presented for the series of complexes $[Ru(HDPA)_n(bpy)_{3-n}]^{2+}$ (**1**) (n = 0–3), $[Ru(DPA)_n(bpy)_{3-n}]^{(2-n)+}$ (**2**) (n = 0–3), and $[Ru(HDPA)_n(DPA)_{3-n}]^{(n-1)+}$ (**3**) (n = 0–3), where HDPA = di-2-pyridylamine, DPA^- = deprotonated dipyridylamine, and bpy = 2,2'-bipyridine. For **1** at −40 °C the voltammetric pattern reveals reversible reduction waves corresponding to the number of coordinated bpy ligands and one irreversible reduction wave for all HDPA-coordinated species at more negative potentials attributed to pyridyl π^* reduction. All species have one reversible oxidation wave corresponding to a metal-localized Ru(III/II) process. For **2** the reduction pattern still corresponds to reversible bpy reduction processes while there are no indications of reduction processes associated with DPA^-. Most notable is the appearance of additional reversible oxidation waves in the potential region from −0.4 to +1.2 V (vs. $Fc^{+/0}$). Three such waves are seen for the n = 2 complex and two for n = 1. The most negative of these waves is shown from ESR results to correspond to a Ru(III/II) couple while the remaining waves involve further metal-localized oxidations and/or DPA^--localized oxidations. For **3** only irreversible reduction waves are seen at very negative potentials. Consistent with the other results is the appearance of an additional oxidation wave for **3** (n = 2). For **1** visible charge-transfer bands indicating transitions from Ru(II) to both the bpy π^* orbitals (~450 nm) and the HDPA pyridyl π^* orbitals (350 nm) are observed. The emission remains $d\pi^*$ from bpy as in the n = 0 complex. For **2** (n = 1 and 2) very low energy charge-transfer transitions (558 and 605 nm, respectively) assigned as $d\pi^*$ (bpy) are seen. The energies of these bands correlate well with the electrochemically predicted values. These results confirm that substantial changes occur in coordinated HDPA on deprotonation, and the results for **2** suggest that a metal–ligand interaction unique to Ru imine complexes exists.

Introduction

Recent photophysical, electrochemical, and electron spin resonance studies, by both these laboratories[1-9] and others,[10-13] conclusively establish that for the majority of nominally d^6 transition-metal complexes of multidentate imine ligands such as $[Ru(bpy)_3]^{2+}$ the lowest excited-state orbital (the orbital from which $d\pi^*$ or $\pi\pi^*$ emission arises in spectroscopy and the redox orbital in electrochemistry) is localized on a single chelate ring (i.e. spatially isolated) with only minimal interligand interaction. The cyclic voltammetric pattern is remarkably similar for all these complexes and has proven very useful in elucidating the single ring nature of the redox orbitals.[3-6,8-10] For the iron group metal polypyridine complexes the voltammetry reveals only one oxidation wave assigned to a metal-localized M(III/II) couple whereas a series of reduction waves is observed in a pattern indicative of sequential addition of one electron into each of the lowest available diimine-localized π^* orbitals followed at more negative potentials by the addition of a second electron into each of these orbitals. With relatively few exceptions there are no intervening heterogeneous charge-transfer kinetic or chemical complications. Furthermore, the voltammetric results provide a valuable complement to the spectroscopic data and can assist in making spectroscopic assignments.[14-16]

(1) DeArmond, M. K.; Carlin, C. M. *Coord. Chem. Rev.* **1981**, *36*, 325.
(2) Carlin, C. M.; DeArmond, M. K. *Chem. Phys. Lett.* **1982**, *89*, 297.
(3) Motten, A. G.; Hanck, K. W.; DeArmond, M. K. *Chem. Phys. Lett.* **1981**, *79*, 541.
(4) Morris, D. E.; Hanck, K. W.; DeArmond, M. K. *J. Am. Chem. Soc.* **1983**, *105*, 3032.
(5) Morris, D. E.; Hanck, K. W.; DeArmond, M. K. *J. Electroanal. Chem. Interfacial Electrochem.* **1983**, *149*, 115.
(6) DeArmond, M. K.; Hanck, K. W.; Morris, D. E.; Ohsawa, Y.; Whitten, D. G.; Neveux, P. E. *J. Am. Chem. Soc.* **1983**, *105*, 6522.
(7) Carlin, C. M.; DeArmond, M. K., to be submitted for publication in *J. Am. Chem. Soc.*
(8) Kahl, J. L.; Hanck, K. W.; DeArmond, M. K. *J. Phys. Chem.* **1978**, *82*, 540.
(9) Kahl, J. L.; Hanck, K. W.; DeArmond, M. K. *J. Phys. Chem.* **1979**, *83*, 2611.
(10) Saji, T.; Aoyagui, S. *J. Electroanal. Chem. Interfacial Electrochem.* **1980**, *110*, 329 and references therein.
(11) Heath, G. A.; Yellowlees, L. J.; Braterman, P. S. *Chem. Phys. Lett.* **1982**, *92*, 646.
(12) Dallinger, R. F.; Woodruff, W. H. *J. Am. Chem. Soc.* **1979**, *101*, 4391.
(13) Bradley, P. G.; Nurit, K.; Hornberger, B. A.; Dallinger, R. F.; Woodruff, W. H. *J. Am. Chem. Soc.* **1981**, *103*, 7441.
(14) Rillema, D. P.; Allen, G.; Meyer, T. J.; Conrad, D. *Inorg. Chem.* **1983**, *22*, 1617.

0020-1669/84/1323-3010$01.50/0 © 1984 American Chemical Society

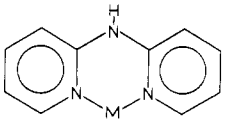

Figure 1. The ligand di-2-pyridylamine (HDPA) with the acidic amine proton shown explicitly. When coordinated to a metal (as shown), the two pyridyl rings are non-coplanar.

In contrast to this uniform behavior are the d⁶ complexes of the bidentate ligand dipyridylamine (HDPA). Unlike α,α'-diimine ligands such as bipyridine and phenanthroline, which are planar and form five-membered rings with the metal (metal heterocycles) on complexation, HDPA is nonplanar and forms six-membered rings when coordinated (Figure 1). In addition, the amine proton of HDPA becomes more acidic on complexation and both the protonated and deprotonated (DPA^-) complexes of cobalt,[17] palladium,[18] and nickel and copper[19] have been studied. The loss of this proton is believed to result in a planar ligand configuration in the complexes.[20] Thus, the ease of deprotonation of the complexes provides for an accessible route to structural and energetic perturbations in these systems.

Recently, the results of an extensive investigation into the absorption and emission properties of the d⁶ series of complexes $[M(HDPA)_n(DPA)_{2-n}Cl_2]^{(n-1)+}$ (M = Ir(III), Rh(III); n = 0–2)[21] and $[Ru(HDPA)_n(DPA)_{3-n}]^{(n-1)+}$ (n = 0–3)[22] were reported. These results indicate that the spectroscopic properties of coordinated HDPA and DPA^- are somewhat different from those of the analogous diimine complexes and require consideration of unusual spectroscopic assignments such as a dd* emission for $[Ru(HDPA)_3]^{2+}$. Subsequent to these findings, an electrochemical study of these complexes was initiated, which further reveals the unique properties associated with coordinated HDPA and DPA^-. This report details these electrochemical results and further spectroscopic data for the Ru(II) complexes of HDPA and DPA^- and the mixed-ligand complexes, $[Ru(HDPA)_n(bpy)_{3-n}]^{2+}$, and the deprotonated analogues.

Experimental Section

Reagents. The complexes $[Ru(HDPA)_3](ClO_4)_2$ and $[Ru(HDPA)_2(DPA)]Cl\cdot nH_2O$ were available from previous work, and synthetic details are described elsewhere.[21,22] The materials used in the preparation of the mixed-ligand complexes of ruthenium were $RuCl_3\cdot nH_2O$ (Engelhard Industries) and di-2-pyridylamine (HDPA) and 2,2'-bipyridine (bpy) from Aldrich Chemical Co. HDPA was recrystallized from benzene and bpy from ethanol prior to use. Tetraethylammonium hexafluorophosphate (TEAH) was prepared from the corresponding chloride by metathesis with KPF_6 and recrystallized twice from water and once from methanol followed by drying in vacuo at 140 °C. Tetrabutylammonium hexafluorophosphate (TBAH) was prepared in the same manner as TEAH from the corresponding bromide salt and recrystallized twice from ethanol. Acetonitrile (Gold Label, Aldrich), *N,N'*-dimethylformamide (Fisher Scientific Co.), and 1,2-dimethoxyethane (Matheson Coleman and Bell) were used as solvents and purified by previously published methods.[6,15] Dimethyl-d_6 sulfoxide (99.9%, Gold Label, Aldrich) was used to prepare the proton NMR samples. Elemental analyses were performed by Atlantic Microlab, Inc.

Syntheses. $[Ru(HDPA)(bpy)_2](ClO_4)_2$ was prepared under an N_2 atmosphere by heating an ethanol solution of $[Ru(bpy)_2Cl_2]$[23] and a slight excess of HDPA at reflux for 4 h.[24] The complex was precipitated by addition of excess aqueous $NaClO_4$, washed with ether, and recrystallized from dry methanol. Anal. Calcd for $[Ru(HDPA)(bpy)_2](ClO_4)_2$: C, 45.98; H, 3.19; N, 12.52. Found: C, 45.98; H, 3.24; N, 12.49.

$[Ru(DPA)(bpy)_2](ClO_4)$ was prepared by adding a twofold excess of 9 M NaOH (aqueous) to a 1:1 H_2O/acetone solution of the purified, protonated precursor. This resulted in the separation of a brown oily layer. A large excess of concentrated aqueous $NaClO_4$ was added, leading to rehomogenation of the solution, and nearly quantitative precipitation of the product occurred within 1 h. The crystals were collected in a Buchner funnel, washed with several portions of cold 1 M NaOH, and immediately transferred to a glovebox.

$[Ru(HDPA)_2(bpy)](ClO_4)_2$ was prepared under an N_2 atmosphere by heating an ethylene glycol solution of $(NH_4)[Ru(bpy)Cl_4]$[25] and a slight excess of HDPA at reflux for 4 h.[26] Precipitation and purification were the same as for $[Ru(HDPA)(bpy)_2](ClO_4)_2$. Anal. Calcd for $[Ru(HDPA)_2(bpy)](ClO_4)_2$: C, 45.11; H, 3.26; N, 14.04. Found: C, 45.22; H, 3.32; N, 14.02.

$[Ru(DPA)_2(bpy)]$ was prepared by adding a large excess of 1 M NaOH (aqueous) to a 6:1 H_2O/acetone solution of the purified, protonated precursor. The resulting solution was heated at 60 °C until precipitation of the uncharged product was complete (~30 min). The crystals were collected in a Buchner funnel, washed with several portins of methanolic NaOH, and immediately transferred to a glovebox. No attempt was made to determine the pK_a values for either of the deprotonated mixed-ligand complexes, but they are believed to be in the same range (10–12) as those for $[Ru(HDPA)_3]^{2+}$ in aqueous solutions.[22]

K(DPA) was prepared by adding potassium metal to a solution of HDPA in rigorously anhydrous dimethoxyethane and stirring at ambient temperature until all metal had reacted. The solvent was vacuum distilled off, leaving a fine yellow precipitate. The precipitate was immediately transferred to a glovebox and washed with several portions of benzene to remove unreacted HDPA.

$K[Ru(DPA)_3]$ was prepared by adding a slight excess of K(DPA) to a dimethoxyethane solution of $[Ru(HDPA)_3]^{2+}$. The red-orange product precipitated immediately. The solvent was then vacuum distilled off and the solid transferred to a glovebox. Subsequent washings with benzene and CH_3CN (in which the solid is only sparingly soluble) were used to remove HDPA, K(DPA), and $KClO_4$ byproducts.

All of the deprotonated species (except $[Ru(HDPA)_2(DPA)]Cl\cdot nH_2O$) were found to be very sensitive to atmospheric moisture. The solids, if allowed to stand exposed to ambient atmosphere, react to produce a wet red-orange solid (presumed to be the reprotonated forms) within 30–60 min. Thus, reliable elemental analyses are not available for the deprotonated products.

$[Ru(bpy)_3](ClO_4)_2$ was prepared and purified by published procedures.[27] No attempts were made to generate or isolate the deprotonated forms of the iridium and rhodium complexes.

Apparatus and Procedure. Electrochemistry. The electrochemical instrumentation used to obtain the voltammetric data has been described in detail elsewhere.[5] Measurements were made in one of the following ways: (1) in a glovebox (N_2 atmosphere) with use of a conventional three-compartment cell with a NaCl salt bridge junction to an aqueous SSCE or (2) in an airtight single-compartment cell under an N_2 atmosphere (into which solvent is vacuum distilled) with use of a silver-wire quasi-reference electrode. The potential of this latter reference electrode was stable enough to remain constant to within ±10 mV over the course of an experiment provided no appreciable electrolysis occurred. Thus, potential values could be referenced to the ferrocene/ferrocenium couple ($E_{1/2}$ = +0.365 V vs. SSCE in 0.1 M TEAH/CH_3CN at room temperature) by adding ferrocene as an internal standard at the end of the experiment. All low-temperature experiments were carried out in the latter cell with

(15) Ohsawa, Y.; Hanck, K. W.; DeArmond, M. K., submitted for publication in *J. Electroanal. Chem. Interfacial Electrochem.*
(16) Saji, T.; Aoyagui, S. *J. Electroanal. Chem. Interfacial Electrochem.* **1975**, *60*, 1.
(17) Johnson, W. L.; Geldard, J. F. *Inorg. Chem.* **1979**, *18*, 664.
(18) Geldard, J. F.; Lions, F. J. *J. Am. Chem. Soc.* **1962**, *84*, 2262.
(19) Hurley, T. J.; Robinson, M. A. *Inorg. Chem.* **1968**, *7*, 33.
(20) Segers, D. P. Ph.D. Thesis, North Carolina State University, in preparation.
(21) Huang, W. L.; Segers, D. P.; DeArmond, M. K. *J. Phys. Chem.* **1981**, *85*, 2080.
(22) Segers, D. P.; DeArmond, M. K. *J. Phys. Chem.* **1982**, *86*, 3768.
(23) Sullivan, B. P.; Salmon, D. J.; Meyer, T. J. *Inorg. Chem.* **1978**, *17*, 3334.
(24) Anderson, S.; Seddon, K. R.; Wright, R. D.; Cocks, A. T. *Chem. Phys. Lett.* **1980**, *71*, 220.
(25) Dwyer, F. P.; Goodwin, H. A.; Gyartas, E. C. *Aust. J. Chem.* **1963**, *16*, 42.
(26) Belser, P.; Zelewsky, A. *Helv. Chim. Acta* **1980**, *63*, 1675.
(27) Palmer, R. A.; Piper, T. S. *Inorg. Chem.* **1966**, *5*, 864.

Table I. Proton NMR Chemical Shifts[a] for Free Ligands and Mixed-Ligand Complexes

	HDPA/DPA⁻					bpy
	H_a	3/3′	4/4′	5/5′	6/6′	3/3′
HDPA	9.9 (s)	8.0 (d)	8.0 (t)	7.2 (t)	8.6 (d)	
DPA⁻	NP[b]	7.3 (d)	7.3 (t)	6.3 (t)	8.0 (d)	
$[Ru(HDPA)_3]^{2+}$	11.1 (s)	8.2 (d)	8.2 (t)	7.3 (t)	7.6 (d)	
$[Ru(HDPA)_2(bpy)]^{2+}$	10.5 (s)			6.6 (t)		8.64 (d)
$[Ru(DPA)_2(bpy)]^0$	NP			5.9 (t)		8.77 (d)
$[Ru(HDPA)(bpy)_2]^{2+}$	10.8 (s)			6.8 (t)		8.7 (d)[c]
$[Ru(DPA)(bpy)_2]^+$	NP			6.0 (t)		8.7 (d)[c]

[a] Chemical shifts are in ppm. Letters in parentheses denote multiplicities: s = singlet; d = doublet; t = triplet. [b] NP = response not present. [c] 3/3′ doublet and triplet assigned to 4/4′ protons on bpy not resolved.

use of a dry ice/isopropyl alcohol bath. Temperatures were monitored external to the sample solution by using a copper–constantan thermocouple with electronic ice point compensation (Omega Engineering, Inc.). In all cases platinum wires were used as working electrodes and counterelectrodes.

Spectroscopy. Room-temperature absorption spectra were measured with a Hitachi Model 110 UV–vis spectrophotometer with 1-cm quartz cells. Emission spectra were obtained with an Aminco-Bowman spectrophotofluorometer. The excitation source was a Hanovia 200-W Hg–Xe lamp, and a Hamamatsu R955 photomultiplier tube was used for detection. Emission spectra were not corrected for PMT or monochromator response. Proton NMR spectra were obtained on a Varian EM-390 90-MHz spectrometer and ESR spectra on a JEOL Co. X-band spectrometer with the same configuration as previously described.[5]

Results

Proton NMR Verification of Deprotonation. To ensure that the products isolated in the deprotonation syntheses are, in fact, the fully deprotonated forms of the precursor complexes and ligand, proton NMR spectra were obtained and compared with the precursor spectra. The well-resolved, characteristic resonances of these species are summarized in Table I. The assignments are based on splitting patterns and chemical shifts and by comparison with the spectra of other d^6 tris(bipyridine) complexes.[28] For all the HDPA-coordinated complexes and the free ligand, the resonance of the acidic amine proton in question is shifted downfield of and well resolved from the aromatic proton resonances. The loss of this resonance (as is observed for all the deprotonated complexes and the free ligand[29]) is, therefore, compelling evidence for the proposed stoichiometry of the deprotonated products.

The complexity of the absorption pattern for the aromatic protons, due to overlapping of the HDPA (DPA⁻) and bipyridine proton resonances and some small changes in symmetry equivalence, precludes a line-for-line assignment and comparison between deprotonated and precursor complexes. Such a comparison is possible for the free ligand (Table I), and all the aromatic proton resonances are shifted upfield for DPA⁻ relative to those for HDPA. A similar shift is easily identified for the highest field signal in the mixed-ligand complexes (assigned to the 5/5′ protons of HDPA and DPA⁻) upon deprotonation and provides further evidence for the proposed composition of the deprotonated products. Solutions of $K[Ru(DPA)_3]$ and $[Ru(HDPA)_2(DPA)]Cl{\cdot}nH_2O$ could not be obtained in sufficient concentrations in any deuterated solvent, so spectra are not available for these products.

Electrochemistry. The cyclic voltammetric results for all of the complexes and the uncomplexed ligands under consideration are summarized in Table II. All results reported are at −40 ± 1 °C, where the voltammetry is relatively uncomplicated. At room temperature in CH_3CN all complexes containing HDPA produce voltammetric responses for the

Table II. Low-Temperature[a] Cyclic Voltammetric Data[b] for HDPA and Mixed-Ligand HDPA and DPA⁻ Complexes

	$E_{1/2}^{c,d}$ (V)				
	3+/2+	2+/1+	1+/0	0/1-	1-/2-
$[Ru(HDPA)_3]^{2+}$	0.53	-2.6[e]			
$[Ru(HDPA)_2(bpy)]^{2+}$	0.51	-1.82	-2.3[e]		
$[Ru(HDPA)(bpy)_2]^{2+}$	0.72	-1.78	-1.97	-2.5[e]	
$[Ru(bpy)_3]^{2+}$	0.85	-1.76	-1.93	-2.14	-2.72[f]
$[Ru(DPA)(bpy)_2]^{1+}$	0.88	0.03	-1.89	-2.11	-2.79
$[Ru(DPA)_2(bpy)]^0$	1.16	0.31	-0.41	-2.06	-2.89
HDPA			0.91[e]	-3.1[e]	
bpy			1.92[h]	-2.50	-3.1[e]

[a] −40 ± 1 °C. [b] Values to the left of the line are for oxidation processes and to the right for reduction processes. [c] Potentials vs. $Fc^{+/0}$ couple. [d] Average of cathodic and anodic peak potentials for reversible couples, peak potential for irreversible waves. [e] Irreversible wave. [f] Data from 0.2 V/s scan. [g] Quasi-reversible; cathodic peak potential is listed. [h] From ref 8; converted to V vs. $Fc^{+/0}$.

reduction processes indicating serious chemical and/or heterogeneous charge-transfer kinetic complications. In addition no reliable voltammograms could be obtained for $K[Ru(DPA)_3]$ in any of the solvents tested because of limited solubility. K(DPA) was very soluble in all solvents but rapidly passivated the platinum electrodes (forming a bright yellow coating).

$[Ru(HDPA)_n(bpy)_{3-n}]^{2+}$. For the series $[Ru(HDPA)_n(bpy)_{3-n}]^{2+}$ the electrochemistry is dominated by the Ru–bpy portion(s) of the complex (Figure 2). In particular, each complex gives $3 - n$ reversible one-electron reduction waves and these are the most positive reduction processes in each case. For the complexes containing coordinated HDPA there is also an irreversible reduction wave observed. For $[Ru(HDPA)_3]^{2+}$ this is the only Faradaic process at negative potentials and occurs just before the end of the solvent window. For the mixed-ligand complexes this wave occurs at potentials more negative than the reversible wave(s) associated with the bpy ligands and distorts the oxidative component(s) of the previous wave(s). In addition, each complex in this series shows a reversible wave at positive potentials associated with the one-electron oxidation of Ru(II). Further, the three HDPA-coordinated complexes have a very broad, irreversible oxidation wave in the region from +1.6 to +2.5 V (vs. $Fc^{+/0}$). This wave is sharpest for the $n = 1$ complex with $E_p - E_{p/2} = 180$ mV and broadens to $E_p - E_{p/2} > 500$ mV for the $n = 3$ complex. Scans allowed to proceed into this potential region also result in distortion of the Ru(III/II) wave. In contrast, $[Ru(bpy)_3]^{2+}$ shows only a flat base line following the Ru(III/II) wave out to the positive potential limit of the solvent.

(28) Kahl, J. L.; Hanck, K. W.; DeArmond, M. K. *J. Inorg. Nucl. Chem.* **1976**, *41*, 495.
(29) The field was scanned from 9 to 13 ppm to ensure such resonances were not merely shifted due to other factors.

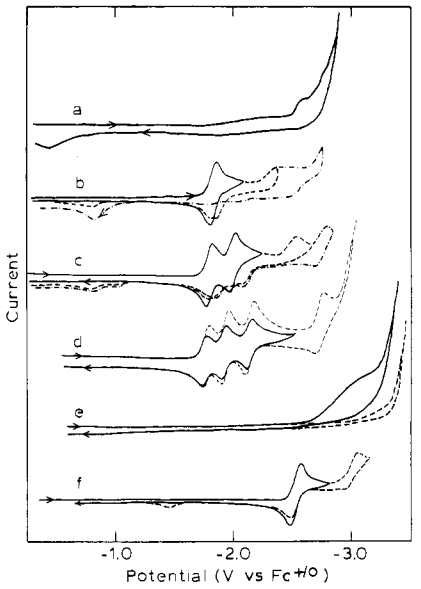

Figure 2. Cyclic voltammograms of $[Ru(HDPA)_n(bpy)_{3-n}](ClO_4)_2$ and the free ligands in 0.1 M TEAH/CH_3CN at −40 ± 1 °C (scan rates 0.1 V/s): (a) $n = 3$; (b) $n = 2$; (c) $n = 1$; (d) $n = 0$ (dashed line, scan rate 0.2 V/s); (e) HDPA; (f) bpy. Dashed line in (e) is 0.1 M TEAH/CH_3CN blank. Concentrations are all ~0.5 mM.

Under these same conditions, uncomplexed bipyridine has a reversible one-electron reduction wave at −2.5 V whereas uncomplexed HDPA has only a broad irreversible reduction wave at more negative potential and an irreversible oxidation wave at positive potential (Table I).

$[Ru(DPA)_n(bpy)_{3-n}]^{(2-n)+}$. The cyclic voltammetric responses for the deprotonated mixed-ligand complexes $[Ru(DPA)_n(bpy)_{3-n}]^{(2-n)+}$ ($n = 2, 1$) are illustrated in Figure 3. At potentials negative of ~−0.5 V the behavior is similar to that of the corresponding protonated species in that $3 - n$ reversible, one-electron reduction wave(s) are seen. However, these waves are shifted negatively by more than 100 mV with respect to the corresponding waves in the protonated complexes (Table I). Furthermore, the additional reduction wave (the second wave for $n = 2$ and the third wave for $n = 1$), while still not completely reversible, is shifted to more negative potential and has the same appearance as the fourth wave of $[Ru(bpy)_3]^{2+}$ (Figure 2). Scans that proceed out to this last reduction wave produce no appreciable distortion of the oxidative component(s) of the preceding wave(s) as is the case for the protonated complexes. The most interesting feature of the voltammetry of the deprotonated species is the appearance of additional reversible oxidation processes at potentials positive of −0.5 V. For the $n = 2$ complex a total of three oxidation waves are seen whereas only two occur for the $n = 1$ complex. Also, in contrast to the protonated complexes, the voltammetric behavior of the deprotonated complexes in CH_3CN at room temperature does not indicate kinetic or chemical complications for the reduction processes. Indeed, two reversible reduction waves are resolved for the $n = 1$ species and one wave is resolved for the $n = 2$ species within the available potential window. The same number of oxidation waves are seen in the room-temperature voltammograms as in the low-temperature work although the most positive waves (third for $n = 2$ and second for $n = 1$) become irreversible at room temperature.

In an effort to determine whether the most negative oxidation wave observed for the $n = 1$ and 2 species corresponds to a metal-centered oxidation similar to that for the Ru(III/II) couple in the $n = 0$ complex, electron spin resonance (ESR) spectra were obtained for the one-electron-oxidation products from bulk electrolysis. The experimental details of this procedure are given elsewhere,[4,5] and the electrolyses were carried out in 0.1 M TBAH/CH_3CN at room temperature. Postelectrolysis cyclic voltammograms verified the chemical stability of the oxidation products. For both $n = 1$ and 2 the ESR signal (obtained at ~−110 °C) is highly anisotropic and greater than 300 G in width.[30] For the $n = 1$ product all three principal **g**-tensor components are observed: $g_1 = 2.12$, $g_2 = 2.05$, and $g_3 = 1.91$. For the $n = 2$ product an axially symmetric signal is observed with $g_\perp = 2.11$ and $g_\parallel = 1.92$. No signal was detected for $[Ru(bpy)_3]^{3+}$ under the same experimental conditions due to fast spin–lattice relaxation effects in this temperature range.

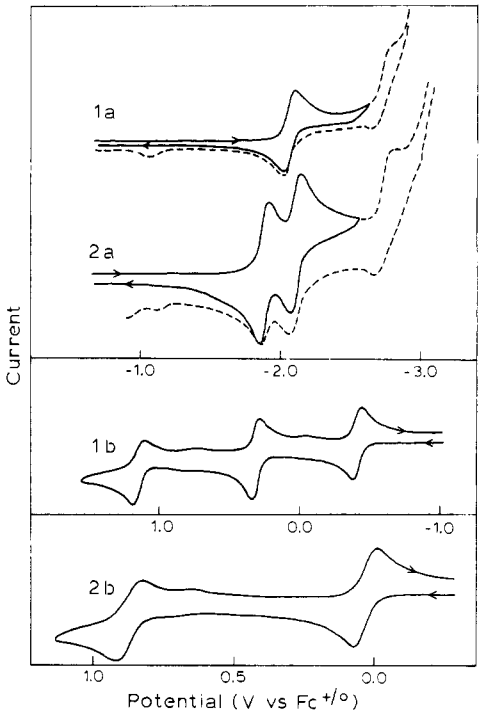

Figure 3. Cyclic voltammograms for the reduction (a) and oxidation (b) processes of $[Ru(DPA)_n(bpy)_{3-n}]^{(2-n)+}$ in 0.1 M TEAH/CH_3CN at −40 ● 2 °C (scan rates 0.1 V/s): (1) $n = 2$; (2) $n = 1$. Concentrations are ~5 mM.

$[Ru(HDPA)_n(DPA)_{3-n}]^{(n-1)+}$. Attempts to study the voltammetry of the various deprotonated forms of the $(HDPA)_3$ complex, $[Ru(HDPA)_n(DPA)_{3-n}]^{(n-1)+}$, met with only limited success. As indicated earlier, the fully deprotonated species ($n = 0$) is easily isolated as a solid but has very limited solubility in electrochemically useful solvents and thus is not amenable to cyclic voltammetric investigation. The mono(deprotonated ligand) complex ($n = 2$) was isolated at pH 11.5 by base addition to an aqueous solution of the purified $n = 3$ complex. However, this material could not be further purified due to the complicated acid/base equilibria involved and likely contains some of the $n = 1$ species. The cyclic voltammetric behavior of this product is illustrated in Figure 4. The only feature here that is distinctly different from the results obtained for the $n = 3$ complex is the presence of additional irreversible oxidation waves at positive potentials. Titration experiments on 0.1 M TEAH/CH_3CN solutions of $[Ru(HDPA)_3]^{2+}$ using DPA^- in CH_3CN as titrant produced results identical with those in Figure 3 after the addition of 1 equiv of DPA^-. However, with further addition of the base the waves become progressively ill-defined.

Spectroscopy. $[Ru(HDPA)_n(bpy)_{3-n}]^{2+}$. Absorption and emission data for the complexes and free ligands are summarized in Table III. The room-temperature absorption spectra of the complexes $[Ru(HDPA)_n(bpy)_{3-n}]^{2+}$ in the visible

(30) Measured from the lowest field peak to the highest field peak.

Table III. Room-Temperature Spectroscopic Data for HDPA and Mixed-Ligand HDPA and DPA⁻ Ruthenium(II) Complexes in CH_3CN

complex	absorption λ_{max}, nm ($10^{-4}\epsilon$, M^{-1} cm^{-1})[a]							emission λ_{max}, nm
$[Ru(HDPA)_3]^{2+}$	250 (3.7)	287 (5.6)	*d*	*d*	375 (sh)[b]	*d*	*d*	*d*
$[Ru(HDPA)_2(bpy)]^{2+}$	245 (3.0)	287 (6.0)	*d*	*d*	353 (1.1)	458 (0.54)	*d*	700 (625)[c]
$[Ru(HDPA)(bpy)_2]^{2+}$	244 (2.3)	288 (5.6)	*d*	*d*	350 (sh)	453 (0.72)	*d*	645 (600)[c]
$[Ru(bpy)_3]^{2+}$	243 (2.2)	287 (>5)	*d*	*d*	*d*	451 (1.2)	*d*	610 (580)[c]
$[Ru(DPA)_2(bpy)]^{0}$ [a]	235 (sh)	293 (6)	315 (sh)	378 (2)	*d*	460 (sh)	605 (0.3)	*e*
$[Ru(DPA)(bpy)_2]^{+}$ [a]	240 (2)	289 (6)	316 (sh)	438 (1)	*d*	493 (sh)	558 (0.3)	*e*
HDPA	265 (1.9)	310 (1.1)	*d*	*d*				
bpy	236 (1.1)	281 (1.4)	*d*	*d*				
DPA^-	261		316	365				

[a] Extinction coefficients are estimated; see text. [b] sh = shoulder. [c] In 4:1 (v/v) EtOH/MeOH at 77 K. [d] Not observed. [e] Results forthcoming.[31]

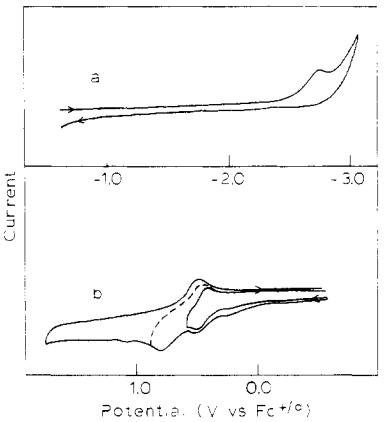

Figure 4. Cyclic voltammograms of 0.5 mM $[Ru(HDPA)_2(DPA)]^+$ in 0.1 M $TEAH/CH_3CN$ at -40 ± 1 °C and 0.1 V/s: (a) reduction; (b) oxidation.

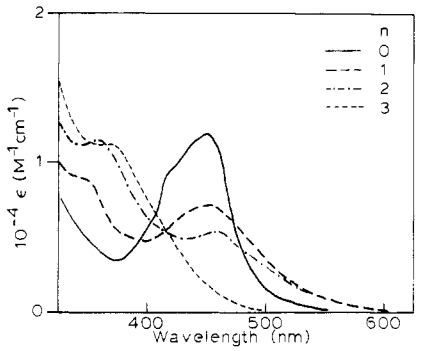

Figure 5. Room-temperature absorption spectra of $[Ru(HDPA)_n(bpy)_{3-n}]^{2+}$ in CH_3CN.

region are shown in Figure 5. These spectra are characterized by two absorption maxima: one centered around 350 nm present only for the HDPA-coordinated species and the other around 450 nm present only for the bpy-coordinated species. As the HDPA ligands are successively replaced by bipyridine, the band at 350 nm decreases in intensity while the band at 450 nm gains intensity. The corresponding room-temperature emissions are observed in the region from 600 to 700 nm with the maximum shifting to higher energy as bpy replaces HDPA. The absorption maxima are approximately constant for this series of complexes in the UV region (Table II), and there is a much larger shift in the energy of these transitions upon complexation for HDPA than for bpy.

$[Ru(DPA)_n(bpy)_{3-n}]^{(2-n)+}$. The room-temperature absorption spectra for the deprotonated complexes $[Ru(DPA)_n(bpy)_{3-n}]^{(2-n)+}$ ($n = 1, 2$) are shown in Figure 6. Because of the difficulty in handling these materials outside of an inert atmosphere, exact solution concentrations (thus ϵ values) are unavailable. Estimates of the extinction coefficients were made from a comparison with the $\pi\pi^*$ bands of the protonated

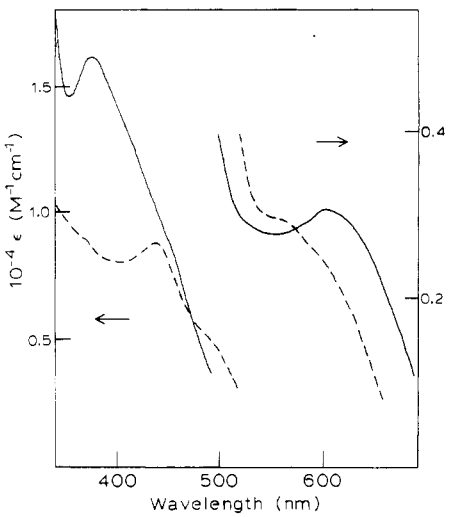

Figure 6. Room-temperature absorption spectra of $[Ru(DPA)_n(bpy)_{3-n}]^{(2-n)+}$ in CH_3CN: (—) $n = 2$; (- - -) $n = 1$.

complexes. The most interesting new features are the appearance of a low-energy, low-intensity band at $\lambda > 550$ nm and a shoulder on the low-energy side of the lowest energy UV band (~315 nm). It is noteworthy that nearly all the bands in the visible region are shifted substantially relative to those of the protonated complexes. Acetonitrile solutions of $K[Ru(DPA)_3]$ could not be made sufficiently concentrated to obtain absorption spectra in the charge-transfer region. However, Me_2SO solutions were possible and the spectrum is nearly the same as the one previously observed for this species in mixed-alcohol solvents.[22] Detailed studies of the emission and emission polarization behavior of the deprotonated mixed-ligand complexes (as well as the protonated precursors) are under way.[31]

Discussion

Electrochemistry. $[Ru(HDPA)_n(bpy)_{3-n}]^{2+}$. The potentials and patterns of the waves for the oxidation and reduction processes of the ruthenium complexes are summarized diagramatically in Figure 7. The low-temperature cyclic voltammetric behavior of the mixed-ligand series $[Ru(HDPA)_n(bpy)_{3-n}]^{2+}$ is consistent with the results obtained for other mono-, bis-, and tris(bipyridine) complexes of d^6 transition metals.[32] The pattern and reversibility of the one-electron-reduction waves clearly indicate that they are associated with the bpy portion of the molecule. The irreversible reduction wave for the HDPA-coordinated complexes at potentials negative of the bpy waves is likely due to the reduction of the

(31) Blakely, R.; Segers, D. P.; DeArmond, M. K., to be submitted for publication in *J. Phys. Chem.*
(32) Vlcek, A. A. *Coord. Chem. Rev.* **1982**, *43*, 39 and references therein.

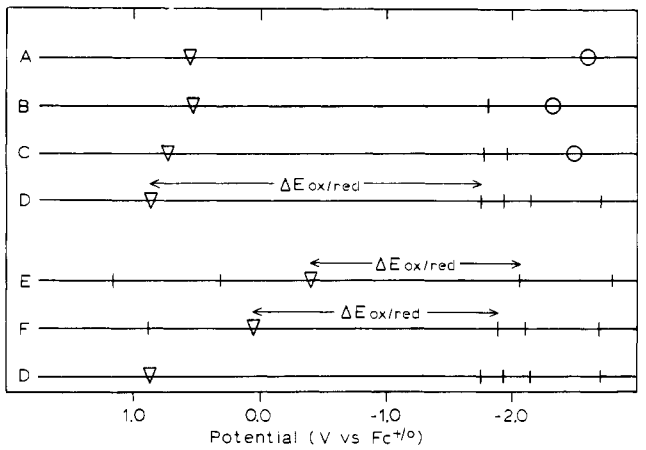

Figure 7. Half-wave potentials for the protonated and deprotonated mixed-ligand complexes in 0.1 M TEAH/CH_3CN at −40 °C: $[Ru(HDPA)_n(bpy)_{3-n}]^{2+}$, (A) $n = 3$, (B) $n = 2$, (C) $n = 1$, (D) $n = 0$; $[Ru(DPA)_n(bpy)_{3-n}]^{(2-n)+}$, (E) $n = 2$, (F) n = 1. ∇ = Ru(III/II) couple; O = irreversible wave associated with HDPA reduction. See text for discussion of ΔE values.

HDPA portion of the complex. Uncomplexed HDPA has a broad irreversible reduction wave at ~−3.1 V (vs. $Fc^{+/0}$). A shift to more positive potentials upon complexation would be expected even for such an irreversible process as a result of the stabilizing influence of the central metal charge.[32] This reduction is thought to primarily involve the pyridyl ring groups and not the amine function on the basis of corroborative spectroscopic evidence discussed below and because of the inherent difficulty in reducing amines.

The reversible one-electron-oxidation waves in the region from 0.5 to 0.9 V for this mixed-ligand series are due to the metal-centered Ru(III/II) couple. The irreversible oxidation wave at 0.91 V for uncomplexed HDPA is thought to be associated with the amine portion of the ligand. Other aromatic amines also show electrochemical activity in this potential region.[33] It is also likely that the broad irreversible activity observed for the HDPA-coordinated complexes in the region from 1.6 to 2.5 V is the result of oxidation primarily involving the amine function. Meyer et al. have recently reported results[34] for a number of aminopyridyl complexes of Ru(II) in which they assign the irreversible wave around 1.2 V (vs. SSCE) to the amine oxidation. However, these amine groups are not part of the immediate coordination sphere. In the HDPA complexes, the amine nitrogen is part of the metal heterocycle. This situation should stabilize the HDPA amine and make the oxidation process more difficult, thus accounting for the positive potential shift on going from free to complexed ligand.

$[Ru(DPA)_n(bpy)_{3-n}]^{(2-n)+}$. The behavior of these deprotonated mixed-ligand complexes is the most interesting result of this work. The observation of multiple reversible oxidation waves for a Ru(II) complex of imine ligands in this potential region is unprecedented. The reversibility at both low and room temperatures and the apparent trend in potential shifts (Figure 7) suggest that the most negative oxidation waves in this series are due to a predominantly metal-localized Ru(III/II) couple. ESR spectroscopy is a sensitive probe for differentiating metal-localized from ligand-localized orbitals, the latter being characterized by narrow lines centered at the free-electron g value ($g_e = 2.0023$). The ESR results for the one-electron-oxidation products of the $n = 1$ and 2 species favor an essentially metal-localized assignment for these first waves since the spectra are quite broad with a relatively large degree of anisotropy, both features indicative of a metal-localized electron configuration ("$(t_2)^5$" in this case).

Somewhat more information can be deduced from these ESR results by consideration of the g values in comparison to those of other iron group d^5 complexes. The spectra obtained for $[M(bpy)_3]^{3+}$ (M = Fe(III), Ru(III), Os(III))[35,36] all have axial symmetry with a very large degree of anisotropy (i.e. the g shifts, $\Delta g = g_i - g_e$, i = ⊥, ∥, are large), and signals are observed only at $T \leq 77$ K due to fast spin–lattice relaxation. These results are consistent with a highly metal-localized ground state. Clearly, this is not the situation for the $[Ru(DPA)_n(bpy)_{3-n}]^{(2-n)+}$ oxidation products since the g shifts are much smaller and signals can be detected even at room temperature. However, behavior remarkably similar to that reported in this study is seen for the d^5 iron group complexes of bidentate sulfur ligands.[37] For these sulfur chelates the small g shifts are accounted for on the basis of a large low-symmetry distortion that results from two effects: (1) a geometric perturbation resulting primarily from the strain inherent in four-membered chelate rings and (2) an electronic perturbation due to increased metal–ligand interaction (higher covalency) as evidenced by the reduction of the Ru(III) spin–orbit coupling constant to 40% of its free-ion value. Similar effects are likely operative in the DPA^- complexes. The geometric distortion would not be the direct result of metal–chelate ring angle strain since the rings are six-membered in the present case, but it is believed[20] that increased interligand steric interactions exist in these complexes so that steric strain could force a distorted geometry. More important is the implication of increased metal–ligand interaction. Such an interaction would help to explain the ability to observe an ESR signal at temperatures well above 77 K. Thus, it is still reasonable to assign the most negative oxidation waves in the DPA^- complexes to a predominantly metal-localized Ru(III/II) couple but the extent of pure metal orbital localization appears to be less than in $[Ru(bpy)_3]^{3+}$.

Of the several possible assignments for the additional oxidation waves (the second wave for $n = 1$ and the second and third waves for $n = 2$) the two most likely are further predominantly metal-localized redox couple(s) (e.g. Ru(III) → Ru(IV) + e^-) and/or predominantly DPA^--localized redox couple(s). The possibility that these waves could be due to bpy π-orbital oxidations can be discounted because Bard et al. have recently shown that these processes occur at much more positive potentials in the $[M(bpy)_3]^{2+}$ complexes[38] and the bpy π-orbital energies are likely not perturbed to such a large extent in these DPA^- complexes. The existence of reversible Ru(IV)/Ru(III) redox chemistry has been demonstrated by Meyer and co-workers for a number of complexes such as $[Ru(bpy)_2(py)O]^{2+}$ (py = pyridine).[39] The Ru(IV) oxidation state is stabilized by the oxo ligand due to the high electron density near the metal center. The increase in electron density associated with deprotonation of HDPA might lead to a similar situation in the present case, particularly in light of the potential shifts observed for the Ru(III/II) couples. However, in DPA^- the additional electron density is probably not as available to stabilize the metal as in the oxo-ligated case. The alternative, namely DPA^--localized couples, could easily result from oxidation(s) involving the essentially nonbonding electrons on the amine nitrogens that are destabilized as a result of deprotonation. Lacking an accurate molecular orbital description, it is impossible to determine which of these two

(33) Bard, A. J.; Faulkner, L. R. "Electrochemical Methods: Fundamentals and Applications"; Wiley: New York, 1980; p 702.
(34) Ellis, C. D.; Margerum, L. D.; Murray, R. W.; Meyer, T. J. *Inorg. Chem.* **1983**, *22*, 1283.
(35) DeSimone, R. E.; Drago, R. S. *J. Am. Chem. Soc.* **1970**, *92*, 2343.
(36) Kober, E. M.; Meyer, T. J. *Inorg. Chem.* **1983**, *22*, 1614.
(37) DeSimone, R. E. *J. Am. Chem. Soc.* **1973**, *95*, 6238.
(38) Gaudiello, J. G.; Sharp, P. R.; Bard, A. J. *J. Am. Chem. Soc.* **1982**, *104*, 6373.
(39) Moyer, B. A.; Meyer, T. J. *Inorg. Chem.* **1981**, *20*, 436.

possibilities is most likely correct.

Finally, it is noteworthy that the irreversible reduction wave observed for the protonated forms of these complexes and associated with the pyridyl moieties is not present for the deprotonated complexes at either low or room temperature. The pattern and potentials of the observed reduction waves are still consistent with occupation of single ring bpy π^* orbitals although there is a distinct shift in the energy of these orbitals relative to the metal oxidation wave as discussed below. Perhaps as important is the implication (from the loss of the irreversible wave) of substantial changes in the geometry and likely the energies of the π^* orbitals of HDPA on deprotonation.

$[Ru(HDPA)_n(DPA)_{3-n}]^{(n-1)+}$. The voltammetric data for the partially deprotonated complex $[Ru(HDPA)_2(DPA)]^+$ (Figure 4) must be interpreted with some caution since neither elemental analysis nor NMR data are available to establish the extent to which extraneous deprotonated species are present. However, the similarity between the voltammograms obtained with the solid material and those from the titration experiments with DPA^- argue in favor of the predominance of the mono DPA^- species. Furthermore, the multiple oxidation processes observed at positive potentials are consistent with the results for the deprotonated mixed-ligand (bpy) complexes.

Spectroscopy. $[Ru(HDPA)_n(bpy)_{3-n}]^{2+}$. The characteristic absorption band at ~450 nm in the spectra of the mixed-ligand complexes $[Ru(HDPA)_n(bpy)_{3-n}]^{2+}$ is similar to that seen for other mixed mixed-ligand polypyridyl complexes of Ru(II)[14,15] and is assigned as metal to ligand charge transfer (MLCT); $d(Ru(III)) \rightarrow \pi^*(bpy)$. There remains some question whether the band at ~350 nm is due to an HDPA ligand-localized transition that is shifted to lower energy on complexation (as with the Co complex[17]) or a MLCT transition from Ru(II) to a π^* orbital on the HDPA pyridyl moieties. Assuming that the irreversible reduction wave observed for all the HDPA complexes is associated predominantly with the pyridyl functions, the electrochemistry supports the MLCT assignment. The occurrence of the voltammetric wave at potentials more negative than the bpy reduction waves indicates that HDPA has vacent (probably π^*) orbitals at higher energy than the bpy π^* orbitals. Thus, one would expect such a MLCT transition at higher energy as is observed. Furthermore, $[Ru(bpy)_2(py)_2]^{2+}$ (cis and trans)[40] and $[Ru^{II}L_5(py)]^{n+}$ complexes[41] show similar absorptions in the region from 330 to 400 nm. The preliminary emission results for this series of complexes indicate that these transitions are essentially MLCT ($d\pi^*$ from bpy^- to Ru(III)) in nature as observed for $[Ru(bpy)_3]^{2+}$.

$[Ru(DPA)_n(bpy)_{3-n}]^{(2-n)+}$. The new low-energy, low-intensity bands observed for these deprotonated complexes are responsible for their unique colors ($n = 2$ is green, $n = 1$ is brown). These transitions are also assigned as MLCT (Ru(II) to bpy). This assignment is based on a relatively simple but generally applicable linear relationship between the half-wave potential separation of the metal-centered oxidation wave and the first ligand reduction wave ($\Delta E_{ox/red}$ in Figure 7) and the energy of the charge-transfer absorption maximum. This relationship is discussed in detail elsewhere.[14,15] The low energies of these absorption bands can be seen to be consistent with the small values of $\Delta E_{ox/red}$ compared to the same quantities for the protonated HDPA mixed-ligand series (Figure 7). The low intensities of these transitions likely reflect the slightly different nature of the d^5 core as noted from the ESR results. The assignment of the remaining visible absorption bands will be considered in detail in a forthcoming report,[31] but at least one of these is certain to result from a DPA^- intraligand transition since uncomplexed DPA^- has what is likely an intraligand charge-transfer transition at 365 nm.

$[Ru(HDPA)_n(DPA)_{3-n}]^{(n-1)+}$. The anticipated usefulness of voltammetric results to corroborate the emission assignments in these deprotonated complexes is seriously hampered by the lack of data on all the various deprotonated forms. However, consideration of the available data including that for the mixed-ligand complexes does enable some conclusions to be drawn. Provided that the trend in potential shifts exhibited in Figure 7 for the mixed-ligand DPA^- complexes continues to be valid for $[Ru(DPA)_3]^-$, the metal-centered oxidation for this ion would be predicted to be at ~−1.0 V (vs. $Fc^{+/0}$). Even if this value is too negative by ~1 V, one cannot rule out the possibility of a $d\pi^*$ charge-transfer emission. The difficulty arises because these metal oxidations are significantly negative of those in other Ru(II) diimine complexes and no DPA^- π^* reductions are observed. However, it is possible that these DPA^- reduction processes lie just negative of the available potential window of CH_3CN. In this case the potential separation, $\Delta E_{ox/red}$, would still be consistent with a MLCT assignment. This assignment seems as reasonable as the previous πd^* ligand to metal charge-transfer assignment[22] since no metal-localized d^* reduction process is observed. Clearly, any assistance from electrochemical data in making a definite assignment for this transition must await the observation of one of these additional electrochemical processes. Furthermore, the πd^* emission assignments for the deprotonated Ir(III) and Rh(III) complexes[22] must be reconsidered for the same reasons.

Summary and Conclusions

The cyclic voltammetric data presented here for complexes containing protonated (HDPA) and deprotonated (DPA^-) dipyridylamine further reveals the unusual properties resulting from complexation of this ligand to d^6 transition metals. The protonated forms show electrochemical behavior typifying the essentially independent functional groups of HDPA with an irreversible reduction at very negative potentials associated with the pyridyl π^* systems and an oxidation of the amine function that is shifted to more positive potentials on complexation due to stabilization in the metal heterocycle. In the mixed-ligand complexes the distinctive bpy reduction pattern is observed although it is severely distorted at room temperature. Charge-transfer absorptions are observed indicating transitions to both the HDPA pyridyl π^* systems and the bpy π^* systems while the emission remains $d\pi^*$ charge transfer from bpy π^* as seen in $[Ru(bpy)_3]^{2+}$.

On deprotonation of the mixed-ligand complexes the bpy reduction pattern remains but is now undistorted at both low and room temperatures. No reduction processes, either reversible or irreversible, can be resolved for the DPA^- coordinated ligand. However, several new oxidation waves appear for these complexes at unusually negative potentials. The most negative of these waves remains the essentially metal-localized Ru(III/II) oxidation as seen in other Ru diimine complexes although the ESR results suggest an increased metal–ligand interaction. The additional oxidation waves result from further metal-localized oxidations or DPA^--localized oxidations or both, but a distinction cannot readily be made without further information regarding the orbital energy ordering (π, n, and π^*) in DPA^-. The low-energy absorption bands observed for these complexes are assigned as MLCT to bpy as with the protonated complexes, and the low energy is reflected by the small potential difference between the metal oxidation and the first bpy reduction wave. The difference observed between these protonated and deprotonated complexes, especially in electrochemical properties, clearly indicates that substantial changes in the structure and

(40) Krause, R. A. *Inorg. Chim. Acta* **1977**, *22*, 209.
(41) Chaisson, D. A.; Hintze, R. E.; Stuermer, D. H.; Peterson, J. D.; McDonald, D. P.; Ford, P. C. *J. Am. Chem. Soc.* **1972**, *94*, 6665.

likely energy result from deprotonation of HDPA as suggested previously. The deprotonated complexes in particular are excellent candidates for more extensive investigation as the low-energy charge-transfer bands and indications of increased metal–ligand interactions make these species unique members of the class of Ru(II) tris(diimine) complexes.

Acknowledgment. We wish to express gratitude to Charles T. Vance of this department for helpful discussions concerning the isolation of K(DPA). This research was supported by NSF Grants CHE-81-19702 and CHE-80-14183.

Registry No. $[Ru(HDPA)_3]^{2+}$, 84052-35-7; $[Ru(HDPA)_2(bpy)]^{2+}$, 91295-39-5; $[Ru(HDPA)(bpy)_2]^{2+}$, 91295-40-8; $[Ru(bpy)_3]^{2+}$, 15158-62-0; $[Ru(DPA)(bpy)_2]^{+}$, 91295-41-9; $[Ru(DPA)_2(bpy)]$, 91295-42-0; $[Ru(HDPA)_3]^{3+}$, 91295-43-1; $[Ru(HDPA)_3]^{+}$, 91295-44-2; $[Ru(HDPA)_2(bpy)]^{3+}$, 91295-45-3; $[Ru(HDPA)_2(bpy)]^{+}$, 91295-46-4; $[Ru(HDPA)_2(bpy)]$, 91295-47-5; $[Ru(HDPA)(bpy)_2]^{3+}$, 91295-48-6; $[Ru(HDPA)(bpy)_2]^{+}$, 91295-49-7; $[Ru(HDPA)(bpy)_2]$, 91295-50-0; $[Ru(HDPA)(bpy)_2]^{-}$, 91295-51-1; $[Ru(bpy)_3]^{3+}$, 18955-01-6; $[Ru(bpy)_3]^{+}$, 56977-24-3; $[Ru(bpy)_3]$, 74391-32-5; $[Ru(bpy)_3]^{-}$, 56977-23-2; $[Ru(bpy)_3]^{2-}$, 87279-34-3; $[Ru(DPA)(bpy)_2]^{2+}$, 91295-52-2; $[Ru(DPA)(bpy)_2]^{3+}$, 91295-53-3; $[Ru(DPA)(bpy)_2]$, 91295-54-4; $[Ru(DPA)(bpy)_2]^{-}$, 91295-55-5; $[Ru(DPA)(bpy)_2]^{2-}$, 91295-56-6; $[Ru(DPA)_2(bpy)]^{+}$, 91295-57-7; $[Ru(DPA)_2(bpy)]^{2+}$, 91295-58-8; $[Ru(DPA)_2(bpy)]^{3+}$, 91295-59-9; $[Ru(DPA)_2(bpy)]^{-}$, 91295-60-2; $[Ru(DPA)_2(bpy)]^{2-}$, 91295-61-3; $[Ru(HDPA)(bpy)_2](ClO_4)_2$, 91295-64-6; $[Ru(bpy)_2Cl_2]$, 15746-57-3; $[Ru(DPA)(bpy)_2](ClO_4)$, 91311-03-4; $[Ru(HDPA)_2(bpy)](ClO_4)_2$, 91295-65-7; $K[Ru(DPA)_3]$, 91295-67-9; K(DPA), 91295-66-8; DPA^{-}, 91295-68-0; HDPA, 1202-34-2; $HDPA^{+}$, 91295-62-4; $HDPA^{-}$, 91382-95-5; bpy, 366-18-7; bpy^{-}, 34475-06-4; bpy^{2-}, 91295-63-5.

Contribution from the Istituto Chimico "Ciamician" dell'Università and Istituto FRAE-CNR, Bologna, Italy

Electron-Transfer Quenching of the Luminescence of Ruthenium and Osmium Polypyridine Complexes by Cobalt(III) Complexes

DIANA SANDRINI,[1a] MARIA TERESA GANDOLFI,[1a] MAURO MAESTRI,[1a,b] FABRIZIO BOLLETTA,[1a,b] and VINCENZO BALZANI*[1a,b]

Received October 24, 1983

The quenching of the luminescence of $Ru(bpy)_3^{2+}$, $Os(phen)_3^{2+}$, and other Ru polypyridine complexes by 17 Co(III) complexes has been studied in aqueous solution. The quenching rate constants correlate with the rate constants available for reduction of the same Co(III) complexes by $Ru(NH_3)_6^{2+}$ or $Cr(bpy)_3^{2+}$, as expected for an electron-transfer quenching mechanism. Conversely, there is no correlation with the rate constants for the quenching of the luminescence of $Cr(bpy)_3^{3+}$, which was previously shown to occur by energy transfer. The rate constants obtained in this paper and other homogeneous data taken from the literature for outer-sphere electron-transfer reactions of $Co(NH_3)_6^{3+}$, $Co(NH_3)_5H_2O^{3+}$, $Co(en)_3^{3+}$, $Co(bpy)_3^{3+}$, and $Co(phen)_3^{3+}$ have been examined by the approach based on the log k_{cor} vs. ΔG plot in an attempt to disentangle the effects of nuclear and electronic terms on the rate constants. This analysis has led to the following values for the electronic transmission coefficient **k** and for the intrinsic barrier $\Delta G^{\ddagger}$ of the self-exchange reactions: $Co(NH_3)_6^{3+}$ and $Co(NH_3)_5H_2O^{3+}$, $\mathbf{k} = 10^{-1\pm1}$, $\Delta G^{\ddagger} = 24 \pm 2$ kcal/mol; $Co(en)_3^{3+}$, $\mathbf{k} = 10^{-3\pm1}$, $\Delta G^{\ddagger} = 17 \pm 2$ kcal/mol; $Co(bpy)_3^{3+}$ and $Co(phen)_3^{3+}$, $\mathbf{k} = 10^{-5\pm1}$, $\Delta G^{\ddagger} = 13 \pm 2$ kcal/mol.

Introduction

Outer-sphere electron-transfer reactions continue to be the object of many theoretical and experimental studies.[2-9] The aim of these studies is to understand the role played by nuclear and electronic factors in determining the observed rate constants and eventually to correlate these factors to fundamental molecular parameters such as chemical composition, geometrical structure, and electric charge.

The behavior of the Co(III)–Co(II) complexes has always been the object of much interest because of two features that are expected to cause very low rate constants:[4-8,10-14] (i) the electron-transfer process involves $\sigma^*(e_g)$ antibonding orbitals with a consequent strong change in the nuclear coordinates; (ii) the electron-transfer process is spin forbidden, and thus it can only occur by mixing of excited-state and ground-state wave functions. Furthermore, recent studies have suggested that orbital-overlap problems might also be responsible for the low rate constants.[8,15-20]

(1) (a) Istituto Chimico "Ciamician". (b) Istituto FRAE-CNR.
(2) Chance, B., De Vault, D. C., Frauenfelder, H., Marcus, R. A., Schrieffer, J. R., Sutin, N., Eds. "Tunneling in Biological Systems"; Academic Press: New York, 1979.
(3) Ulstrup, J. "Charge Transfer Processes in Condensed Media"; Springer-Verlag: West Berlin, 1979.
(4) Cannon, R. D. "Electron Transfer Reactions"; Butterworths: London, 1980.
(5) Sutin, N. *Acc. Chem. Res.* **1982**, *15*, 275.
(6) Rorabacher, D. B., Endicott, J. F., Eds. "Mechanistic Aspects of Inorganic Reactions"; American Chemical Society: Washington, DC, 1982; ACS Symp. Ser. No. 198.
(7) Sutin, N. *Prog. Inorg. Chem.* **1983**, *30*, 441.
(8) Endicott, J. F.; Kumar, K.; Ramasani, T.; Rotzinger, F. P. *Prog. Inorg. Chem.* **1983**, *30*, 141.
(9) Balzani, V.; Scandola, F. In "Energy Resources by Photochemistry and Catalysis"; Grätzel, M., Ed.; Academic Press: New York, 1983; Chapter 1, p 1.
(10) Sutin, N. In "Bioinorganic Chemistry"; Eichhorn, G. L., Ed.; American Elsevier: New York, 1973; Vol. 2, Chapter 19, p 611.
(11) Chou, M.; Creutz, C.; Sutin, N. *J. Am. Chem. Soc.* **1977**, *99*, 5615.
(12) Buhks, E.; Bixon, M.; Jortner, J.; Navon, G. *Inorg. Chem.* **1979**, *18*, 2014.
(13) Endicott, J. F.; Durham, B.; Glick, D. M.; Anderson, T. J.; Kuszaj, J. M.; Schmonsees, W. G.; Balakrishnan, K. P. *J. Am. Chem. Soc.* **1981**, *103*, 1431.
(14) Endicott, J. F.; Durham, B.; Kumar, K. *Inorg. Chem.* **1982**, *21*, 2437.
(15) Endicott, J. F.; Heeg, M. J.; Gaswick, D. C.; Pyke, S. *J. Phys. Chem.* **1981**, *85*, 1777.
(16) Buhks, E.; Wilkins, R. G.; Isied, S. S.; Endicott, J. F. In ref 6, p 213.

0020-1669/84/1323-3017$01.50/0 © 1984 American Chemical Society